Electronic Supplementary Material (ESI) for Materials Chemistry Frontiers.

Supplementary Materials

Co_3Fe_7 nanoparticles encapsulated in porous nitrogen-doped carbon nanofiber as bifunctional electrocatalysts for rechargeable zinc-air battery

Miaomiao Liu, Yulong He and Jintao Zhang *

Key Laboratory for Colloid and Interface Chemistry, Ministry of Education, School of Chemistry and Chemical Engineering, Shandong University, Jinan 250100, China

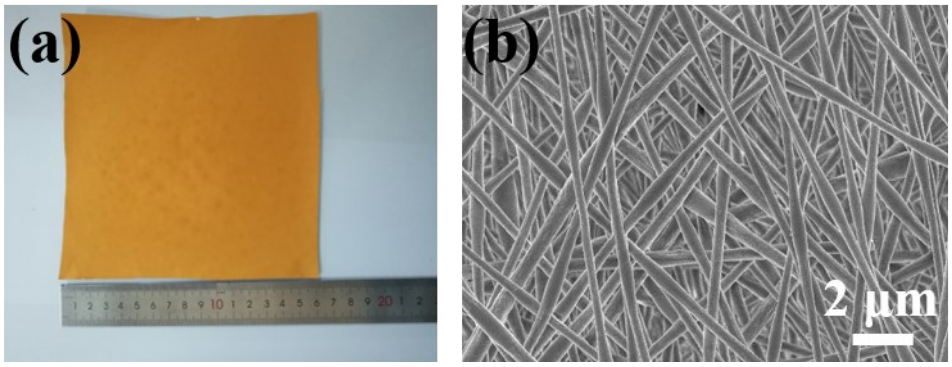

Fig. S1 (a) Digital photo and (b) SEM images of the electrospun nanofiber film.

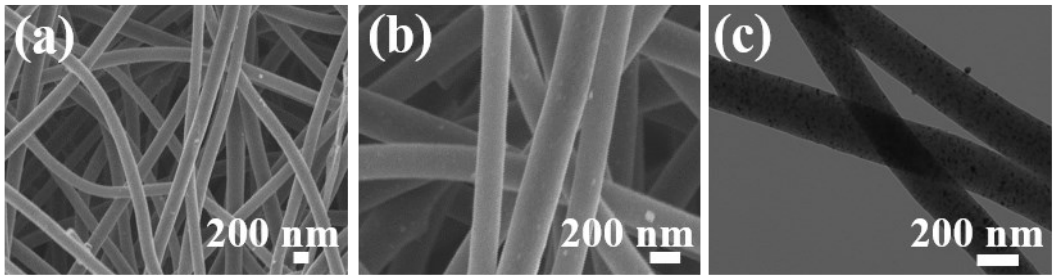

Fig. S2 (a, b) SEM images, (c) TEM image of Co_3Fe_7-CNF-850.

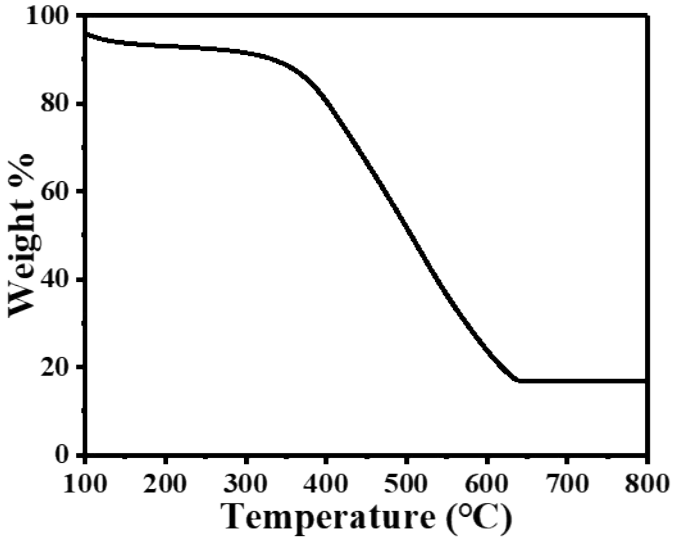

Fig. S3 TG curves of Co_3Fe_7-PVP fibers in N_2.

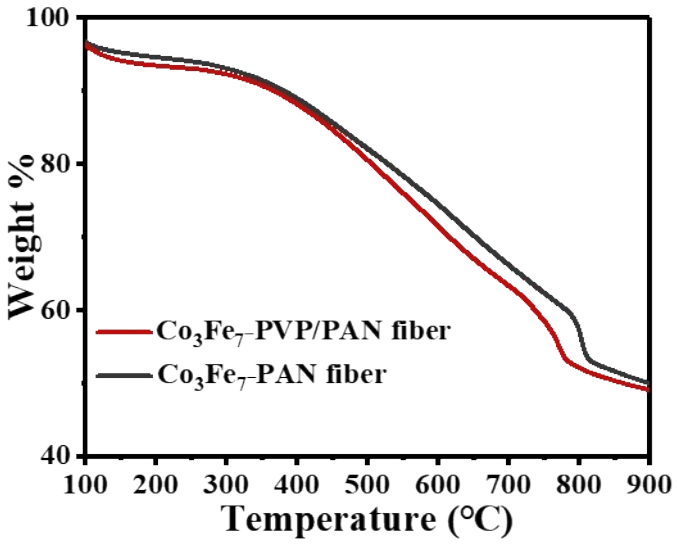

Fig. S4 TG curves of Co_3Fe_7-PVP/PAN fiber and Co_3Fe_7-PAN fiber in N_2.

The non-woven CNFs network is prepared through electrospinning the PVP/PAN solution. As demonstrated in Fig. S3, electrospun PVP fibers decomposed from 310℃ to 620℃. Electrospun PVP-PAN fiber also shows obvious decomposition step between 310℃ and 750℃. Compared with PAN fibers, PVP/PAN fiber shows larger weight less and faster pyrolysis rate. It is not only due to the evolution of gaseous product such as HCN, NH_3 and CO_2, but the decomposition of PVP, resulted in porous structure[1,2].

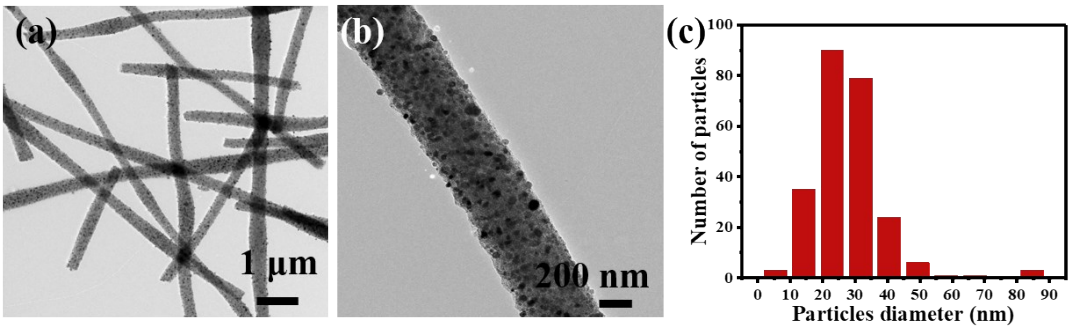

Fig.S5 (a, b) TEM images of Co_3Fe_7-PCNF-850. (c) shows the particle size distribution of Co_3Fe_7 nanoparticles(b).

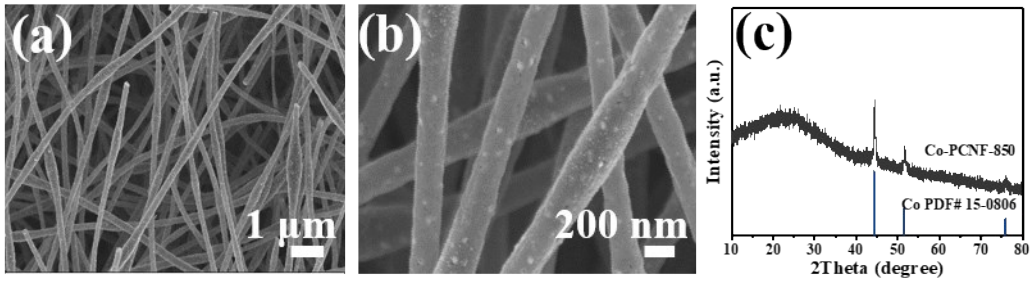

Fig. S6 (a, b) SEM images of Co-PCNF-850, (c) XRD patterns of Co-PCNF-850.

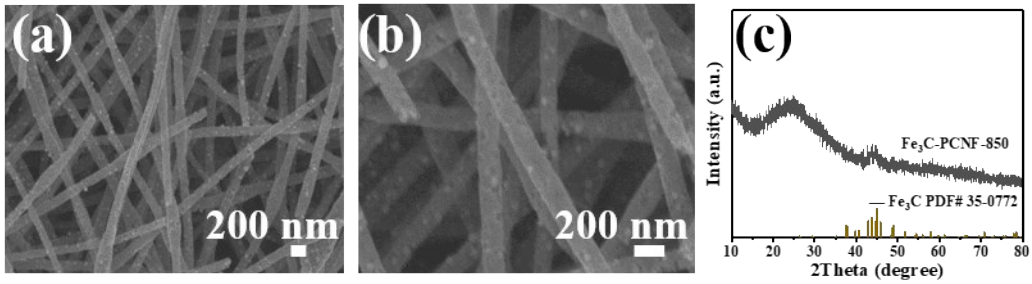

Fig. S7 (a, b) SEM images of Fe_3C-PCNF-850, (c) XRD patterns of Fe_3C-PCNF-850.

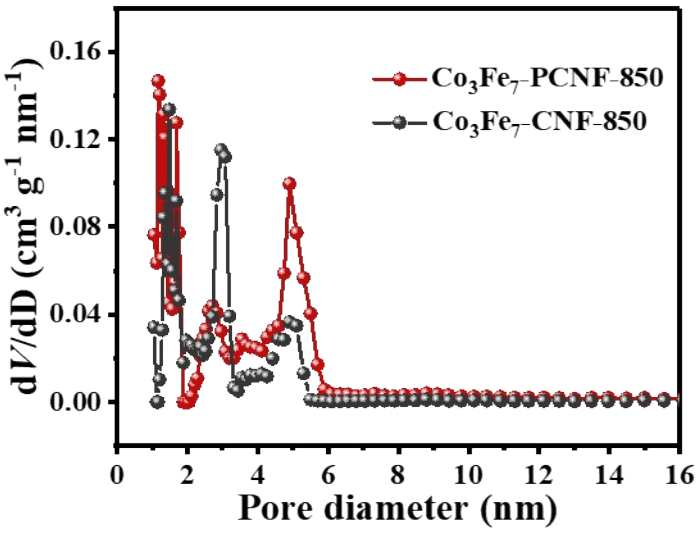

Fig. S8 Pore size distribution of Co_3Fe_7-PCNF-850 and Co_3Fe_7-CNF-850.

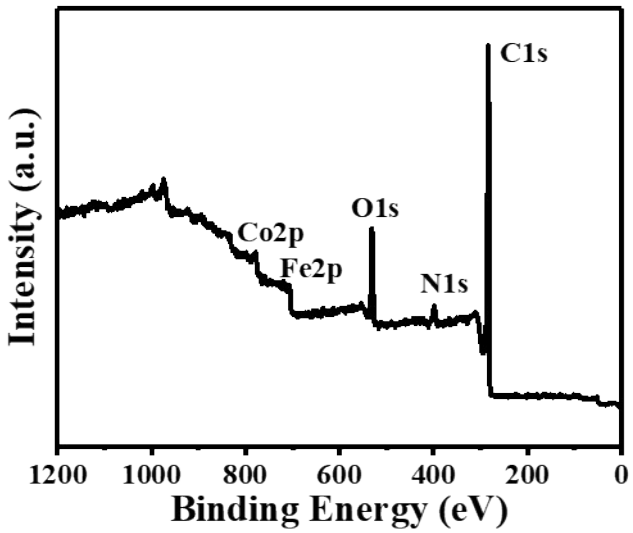

Fig. S9 Survey XPS spectra of Co_3Fe_7-PCNF-850.

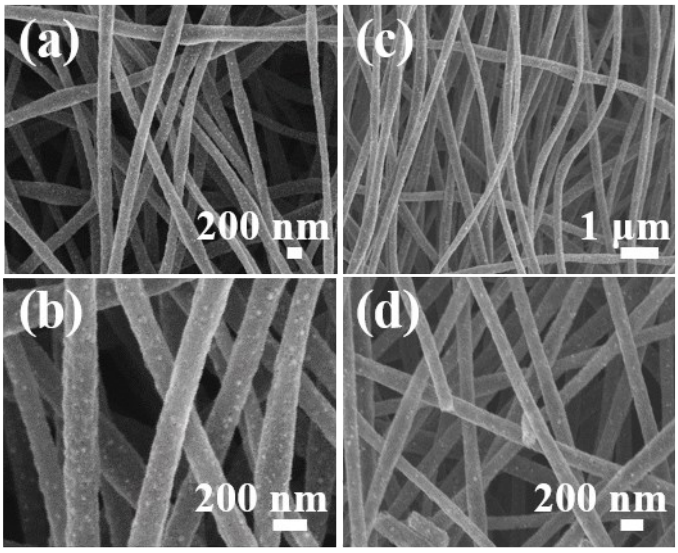

Fig. S10 (a, b) SEM images of Co_3Fe_7-PCNF-800, (c, d) SEM images of Co_3Fe_7-PCNF-900.

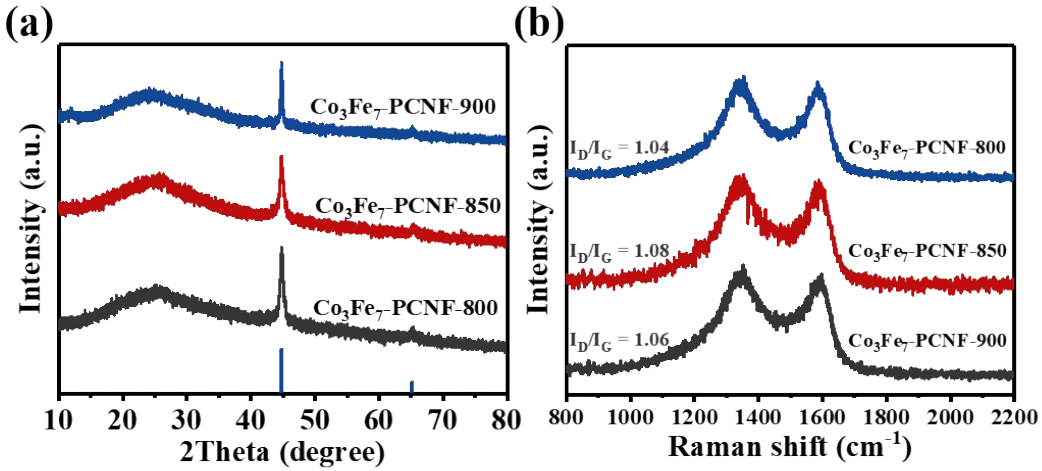

Fig. S11 (a) XRD patterns; (b) Raman spectra of electrocatalysts with different temperatures.

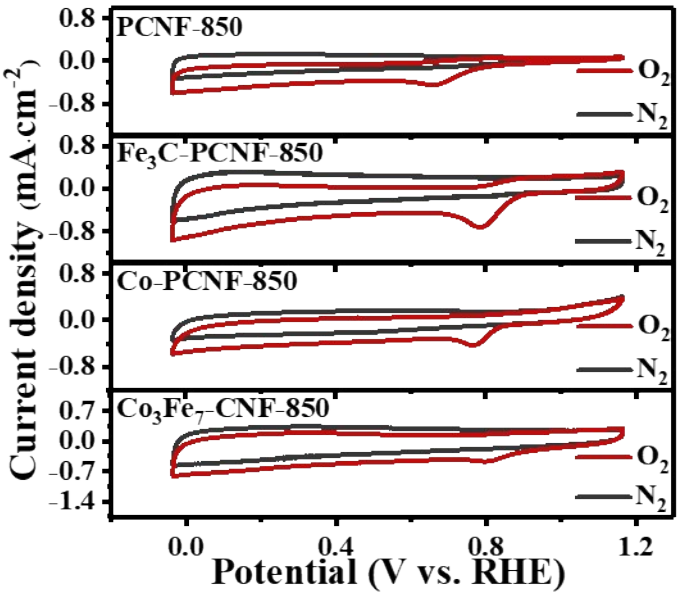

Fig. S12 Cycle voltammetry curves in 0.1 M KOH saturated with N_2 or O_2.

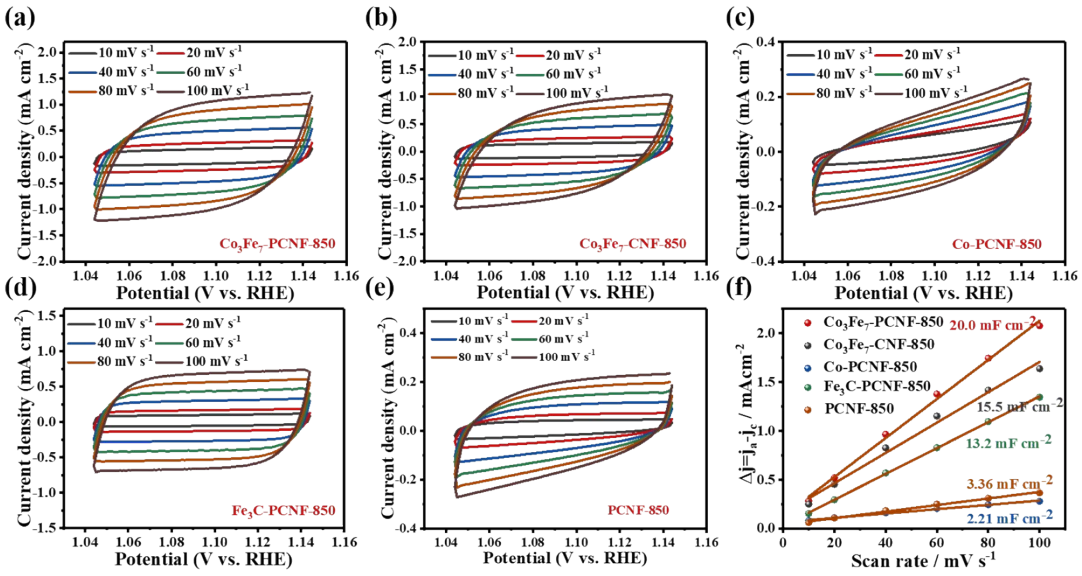

Fig. S13 (a-e) CVs at different scan rates of catalysts and (f) the corresponding C_{dl}.

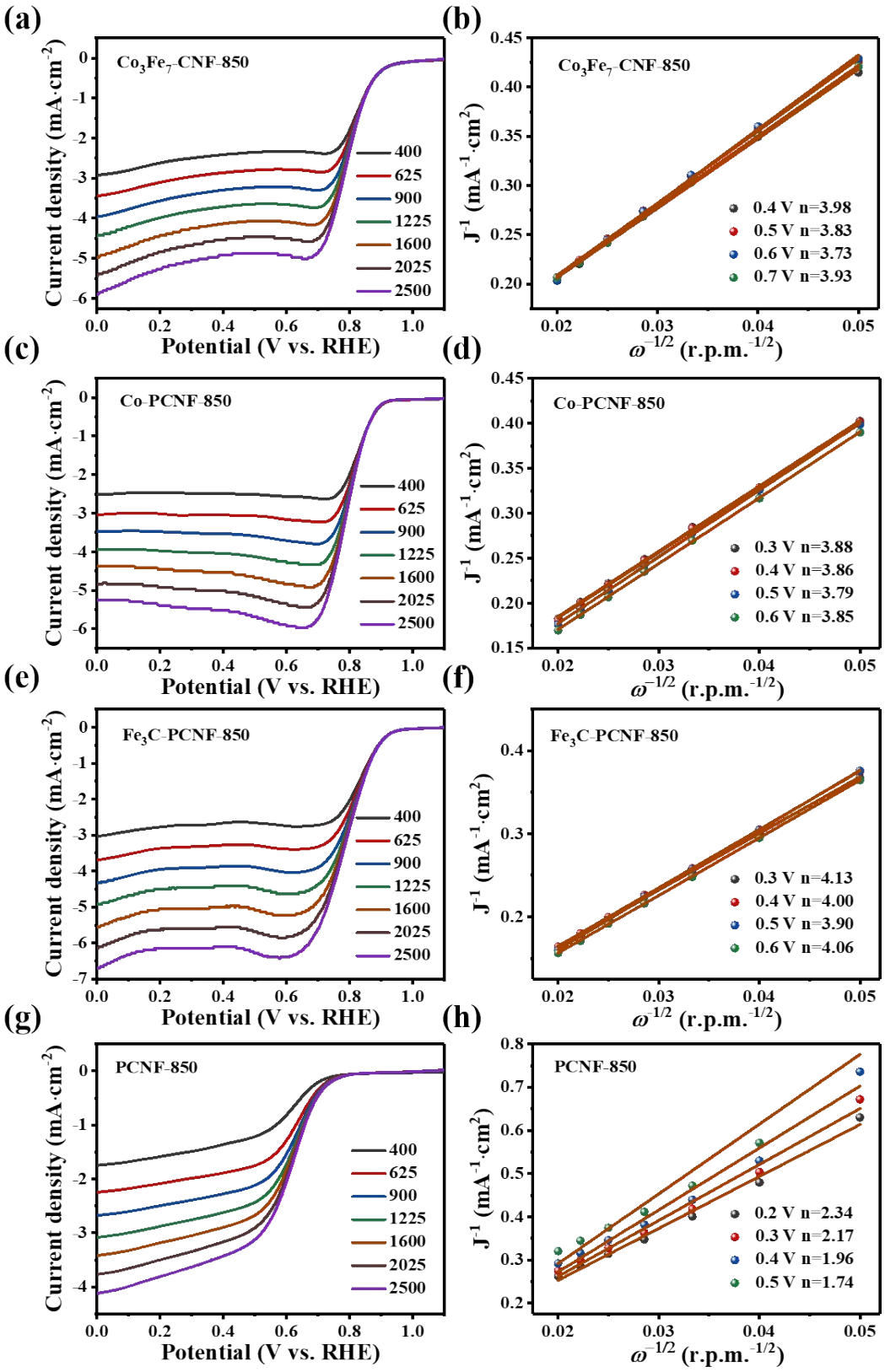

Fig. S14 LSV curves of catalysts in O_2-saturated 0.1 M KOH solution under different rotating speeds and their corresponding K-L plots.

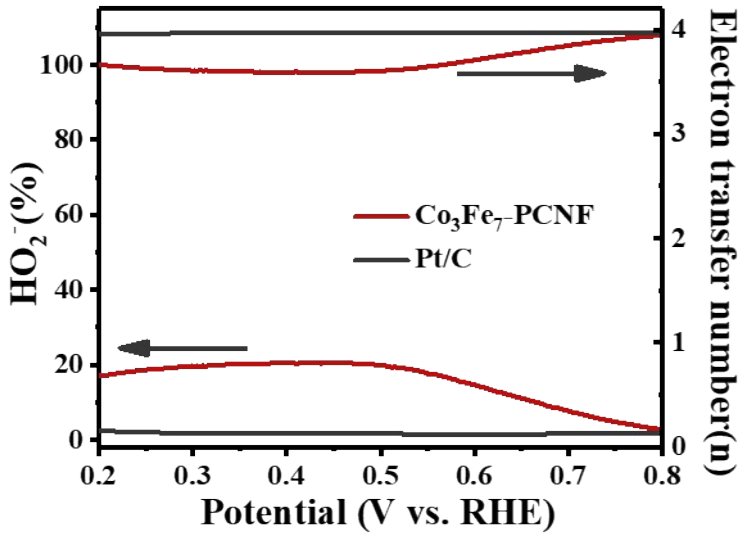

Fig. S15 HO_2^- yield and the corresponding electron transfer number (n) of Co_3Fe_7-PCNF-850 and Pt/C.

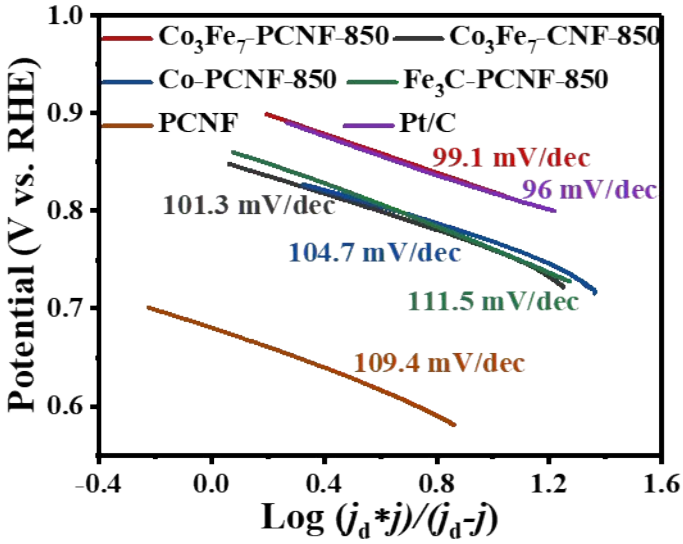

Fig. S16 the corresponding ORR tafel plots.

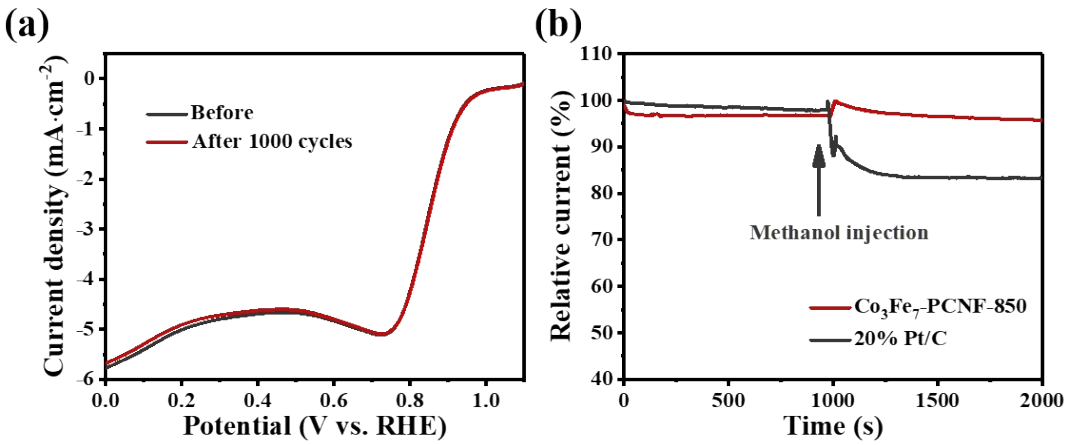

Fig. S17 (a) LSV curves of Co_3Fe_7-PCNF-850 before and after 1000 cycles cyclic voltammetry test; (b) Chronoamperometric response at 0.4 V vs. RHE after the introduction of 2 M methanol solution into 0.1 M KOH solution.

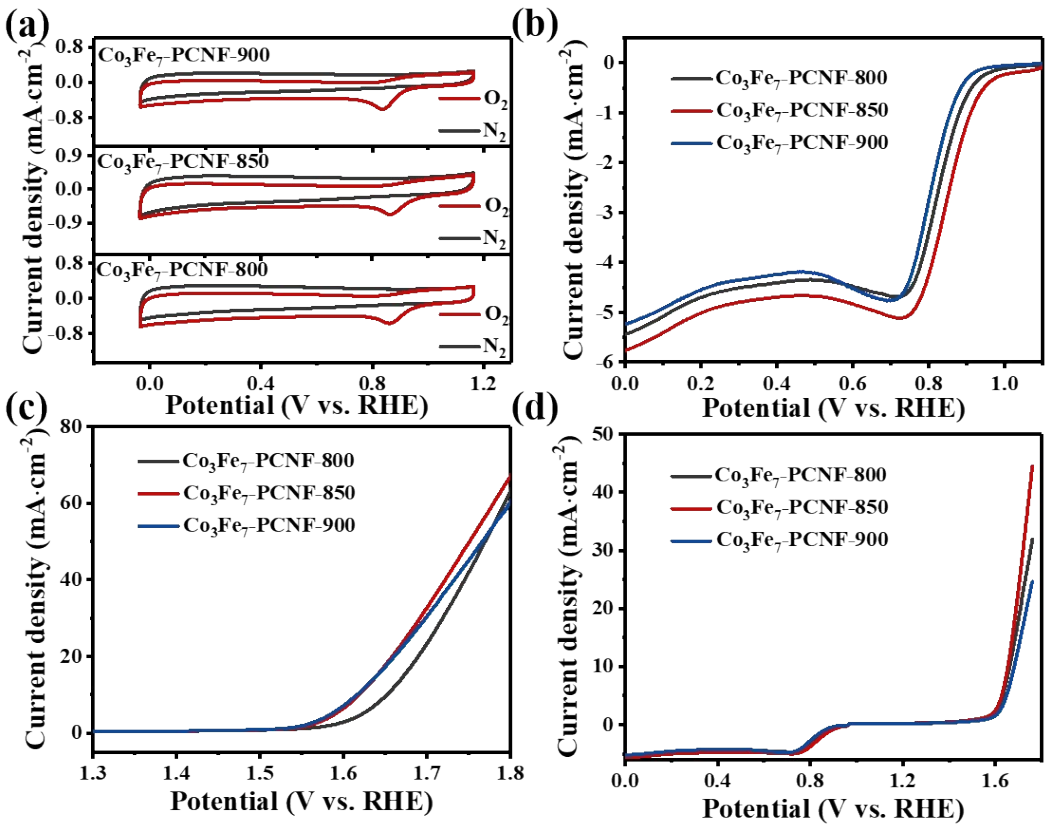

Fig. S18 Electrochemical performance of different temperature products. (a) CV curves in N_2 or O_2 saturated 0.1 M KOH solution. (b) LSV polarization curves for ORR (1600 rpm). (c) LSV polarization curves for OER. (d) Overall Polarization curves of as-prepared catalysts for bifunctional catalytic activity.

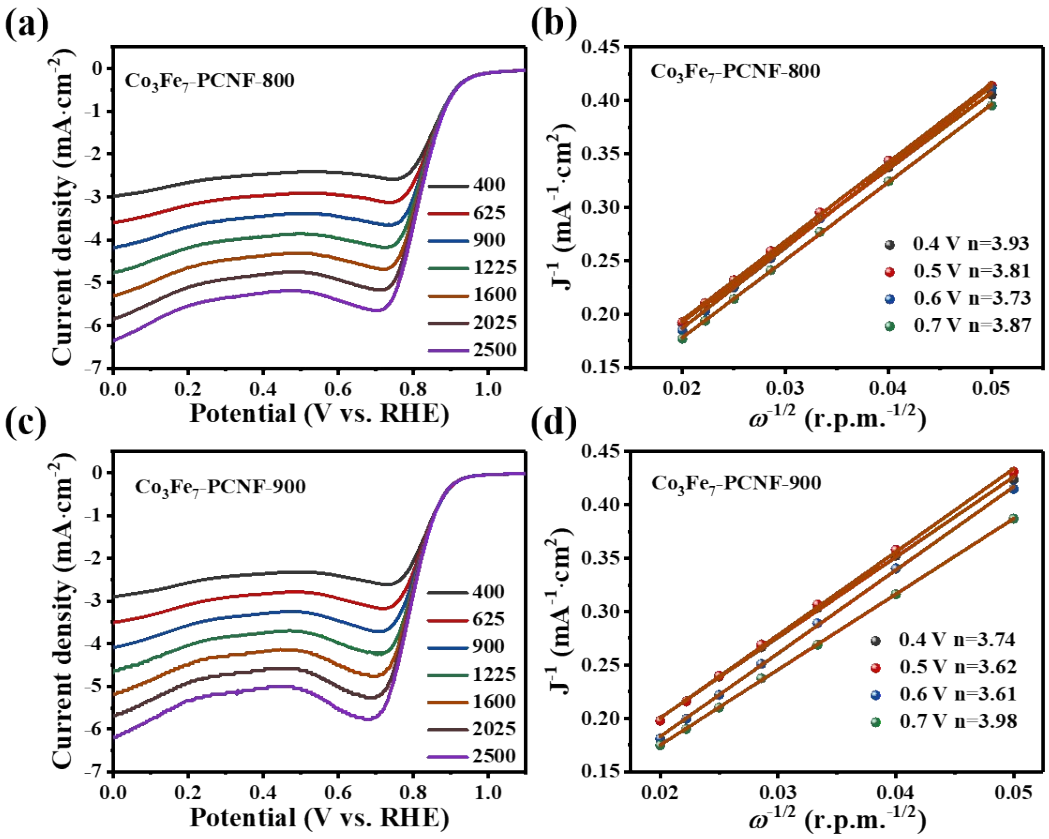

Fig. S19 LSV curves of catalysts in O_2-saturated 0.1 M KOH solution under different rotating speeds and their corresponding K-L plots.

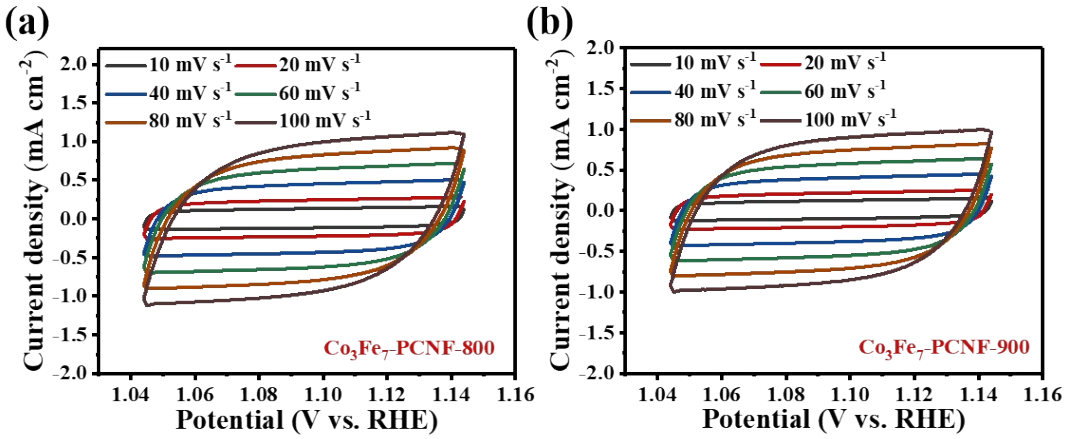

Fig. S20 (a, b) CVs at different scan rates of catalysts and (f) the corresponding C_{dl}.

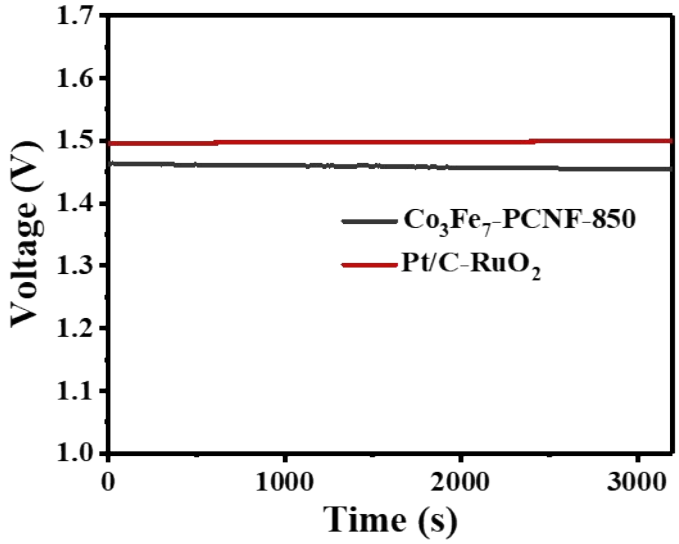

Fig. S21 Open-circuit potential of Co_3Fe_7-PCNF-850 assembled liquid zinc air battery.

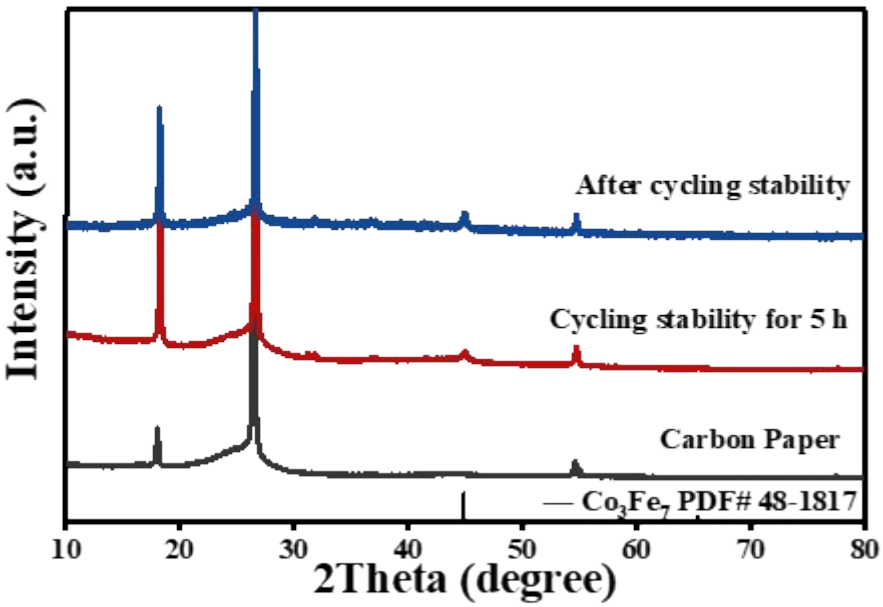

Fig. S22 XRD patterns of Co_3Fe_7-PCNF-850 based battery after cycling stability.

Table S1 Summary of ORR and OER activity of catalysts reported in the literature.

Electrocatalyst	$E_{1/2}$ (V vs. RHE)	$E_{\eta=10}$ (V vs. RHE)	ΔE ($E_{\eta=10}$-$E_{1/2}$) (V vs. RHE)	Ref.
Co_3Fe_7-PCNF-850	**0.83**	**1.61**	**0.78**	**This work**
N-GCNT/FeCo-3	**0.81**	**1.73**	**0.81**	[3]
Co_3Fe_7/NGNRs	**0.80**	**1.58**	**-**	[4]
Co-Co_3O_4@NAC	**0.795**	**1.61**	**0.815**	[5]
(Fe, Co, Ni)$_9S_8$/NSCFs	**0.82**	**1.62**	**0.8**	[6]
FeCo-NGS	**0.80**	**1.61**	**0.81**	[7]
Co@NPCFs	**0.66**	**1.63**	**0.97**	[8]
2D Fe-NG	**0.86**	**1.62**	**0.76**	[9]
3D Fe/N-G	**0.85**	**1.62**	**0.77**	[10]

Table S2 Performance comparison of the liquid zinc air batteries with various electrocatalysts

Electrocatalyst	Open circuit potential (V)	Peak power density (mW cm^{-2})	Current Density (mA cm^{-2})	Cycling stability	Ref.
Co_3Fe_7-PCNF	1.49	213	5	300 h (900 cycles)	This work
Co-Co_3O_4@NAC	1.45	164	5	35 h	[5]
(Fe, Co, Ni)$_9S_8$/NSCFs	1.48	158	10	360 cycles	[6]
Co@NPCFs	1.44	91.9	5	80 h (480 cycles)	[8]
2D Fe-NG	1.51	235.2	12	80 h (480 cycles)	[9]
FeNC-Fe_xC/Fe	1.41	149.4	2	380 cycles	[11]
CoNC	-	181.3	5	110 h (1320 cycles)	[12]
FeNPC	1.51	233.2	3	15 h	[13]
FeNi-NC	-	80.8	8	23 h	[14]
Co-N-Cs	-	158	10	55 h	[15]

References

1. M. S. A. Rahaman, A. F. Ismail, A. Mustafa, A review of heat treatment on polyacrylonitrile fiber, *Polym. Degrad. Stab.*, 2007, **92**, 1421-1432.
2. T. S. He, Y. R. Fu, X. L. Meng, X. D. Yu, X. L. Wang, A novel strategy for the high performance supercapacitor based on polyacrylonitrile-derived porous nanofibers as electrode and separator in ionic liquid electrolyte, *Electrochim. Acta*, 2018, **282**, 97-104.
3. C. Y. Su, H. Cheng, W. Li, Z. Q. Liu, N. Li, Z. F. Hou, F. Q. Bai, H. X. Zhang, T. Y. Ma, Atomic modulation of FeCo-nitrogen-carbon bifunctional oxygen electrodes for rechargeable and flexible all-solid-state Zinc-air battery, *Adv. Energy Mater.*, 2017, **7**, 1602420.
4. J. Joy, S. Rajappa, V. K. Pillai, S. Alwarappan, Co_3Fe_7/nitrogen-doped graphene nanoribbons as bi-functional electrocatalyst for oxygen reduction and oxygen evolution, *Nanotechnology*, 2018, **29**, 415402.
5. X. W. Zhong, W. Yi, Y. Qu, L. Zhang, H. Bai, Y. Zhu, J. Wan, S. Chen, M. Yang, L. Huang, M. Gu, H. Pan, B. Xu, Co single-atom anchored on Co_3O_4 and nitrogen-doped active carbon toward bifunctional catalyst for zinc-air batteries, *Appl. Catal.B-Environ.*, 2020, **260**, 118188.
6. D. P. Jiang Tong Zhou, Zhang Wen, Wu Ming Zai, Fish bone-derived N, S co-doped interconnected carbon nanofibers network coupled with (Fe, Co, Ni)$_9S_8$ nanoparticles as efficient bifunctional electrocatalysts for rechargeable and flexible all-solid-state Zn-air battery, *Electrochim. Acta*, 2021, **373**, 137903.
7. C. Chen, Y. F. Li, D. Cheng, H. He, K. B. Zhou, Graphite nanoarrays-confined Fe and Co single-atoms within graphene sponges as bifunctional oxygen electrocatalyst for ultralong lasting zinc-air battery, *ACS Appl. Mater. Interfaces*, 2020, **12**, 40415-40425.
8. Y. S. Chen, W. H. Zhang, Z. Y. Zhu, L. L. Zhang, J. Y. Yang, H. H. Chen, B. Zheng, S. Li, W. N. Zhang, J. S. Wu, F. W. Huo, Co nanoparticles combined with nitrogen-doped graphitic carbon anchored on carbon fibers as a self-standing air electrode for flexible zinc-air batteries, *J. Mater. Chem. A*, 2020, **8**, 7184-7191.
9. C. Wang, Y. P. Liu, Z. F. Li, L. K. Wang, X. L. Niu, P. Sun, Novel space-confinement synthesis of two-dimensional Fe, N-codoped graphene bifunctional oxygen electrocatalyst for rechargeable air-cathode, *Chem. Eng. J.*, 2021, **411**, 128492.
10. C. Wang, Z. F. Li, L. K. Wang, X. L. Niu, S. W. Wang, Facile synthesis of 3D Fe/N codoped mesoporous graphene as efficient bifunctional oxygen electrocatalysts for rechargeable zn-air batteries, *ACS Sustain. Chem. Eng.*, 2019, **7**, 13873-13885.
11. Y. Y. Qiao, P. F. Yuan, Y. F. Hu, J. N. Zhang, S. C. Mu, J. H. Zhou, H. Li, H. C. Xia, J. He, Q. Xu, Sulfuration of an Fe-N-C Catalyst Containing Fe_xC/Fe Species to Enhance the Catalysis of Oxygen Reduction in Acidic Media and for Use in Flexible Zn-Air Batteries, *Adv. Mater.*, 2018, **30**, 1804504.
12. H. J. Son, M. J. Kim, S. H. Ahn, Monolithic Co-N-C membrane integrating Co atoms and clusters as a self-supporting multi-functional electrode for solid-state zinc–air batteries and self-powered water splitting, *Chem. Eng. J.*, 2021, **414**, 128739.
13. X. F. Zhu, X. Tan, K. H. Wu, C. L. Chiang, Y. C. Lin, Y. G. Lin, D. W. Wang, S. Smith, X. Y. Lu, R. Amal, N,P co-coordinated Fe species embedded in carbon hollow spheres for oxygen electrocatalysis, *J. Mater. Chem. A*, 2019, **7**, 14732-14742.
14. L. Yang, X. F. Zeng, D. Wang, D. P. Cao, Biomass-derived FeNi alloy and nitrogen-codoped

porous carbons as highly efficient oxygen reduction and evolution bifunctional electrocatalysts for rechargeable Zn-air battery, *Energy Storage Mater.*, 2018, **12**, 277-283.

15. S. M. Chen, L. T. Ma, S. L. Wu, S. Y. Wang, Z. B. Li, A. A. Emmanuel, M. R. Huqe, C. Y. Zhi, J. A. Zapien, Uniform Virus-Like Co-N-Cs Electrocatalyst Derived from Prussian Blue Analog for Stretchable Fiber-Shaped Zn-Air Batteries, *Adv. Funct. Mater.*, 2020, **30**, 1908945.